On the stochastic behaviors of locally confined particle systems

Yao Li

Citation: Chaos **25**, 073121 (2015); doi: 10.1063/1.4927300
View online: http://dx.doi.org/10.1063/1.4927300
View Table of Contents: http://scitation.aip.org/content/aip/journal/chaos/25/7?ver=pdfcov
Published by the AIP Publishing

On the stochastic behaviors of locally confined particle systems

Yao Li[a)]
Courant Institute of Mathematical Sciences, New York University, New York, New York 10012, USA

(Received 27 April 2015; accepted 13 July 2015; published online 30 July 2015)

We investigate a class of Hamiltonian particle systems and their stochastic behaviors. Using both rigorous proof and numerical simulations, we show that the geometric configuration can qualitatively change key statistical characteristics of the particle system, which are expected to be retained by stochastic modifications. In particular, whether a particle system has an exponential mixing rate or a polynomial mixing rate depends on whether the geometric setting allows a slow particle being reached by adjacent fast particles. © *2015 AIP Publishing LLC*.
[http://dx.doi.org/10.1063/1.4927300]

The derivation of Fourier's law from microscopic Hamiltonian principles is a major challenge to mathematicians and physicists for the past over a century. Due to the significant difficulty of studying deterministic Hamiltonian models, one important approach is to approximate chaotic Hamiltonian dynamics by stochastic processes. This paper is devoted to investigate statistical properties and stochastic approximations of a billiard-like microscopic heat conduction model proposed by Bunimovich *et al.*[4] We point out that the geometry of the deterministic billiard-like model could lead to a slow rate (polynomial) of mixing, which was overlooked by many early studies. Through a series of analytical and numerical studies, we demonstrate the limitation of the stochastic approximation that comes from some early studies. In addition, we propose new rules of stochastic approximations and verified them numerically.

I. INTRODUCTION

Heat conduction in solids has been intensively studied since the time of Joseph Fourier. For over a century, a major challenge in statistical mechanics is the derivation of macroscopic heat conduction laws like Fourier's law from Hamiltonian microscopic dynamics. Up to now, limited rigorous results are known about Hamiltonian heat conduction models.[2,33] On the other hand, it is well known to mathematicians and physicists that chaotic dynamics produce similar statistics as stochastic processes (see Refs. 3, 7, 8, 12, 26, 32, 36, 38, and references therein). Therefore, one modification is to randomize certain quantities and to turn deterministic Hamiltonian dynamics into stochastic Markovian dynamics while preserving key statistical properties.[9,24,30] In this paper, we address the behavior of stochastic modifications of a class of locally confined interacting particle models. The main goal of this paper is to illustrate that geometric configurations of deterministic models can fundamentally change many statistical characteristics, which are supposed to be retained by their stochastic modifications.

Consider the following microscopic (Hamiltonian) model for heat conduction, which is formed by a chain (or a lattice) of locally confining cells in $\mathbb{R}^2$ like the one shown in Figure 1. Each cell contains an identical rigid disk-shaped particle. The diameter of the particle prevents it from passing through the "bottleneck" between adjacent cells, but particles can collide with their neighbors. Therefore, despite the absence of mass transport, kinetic energy can still be transported through particle-particle collisions. In addition, we assume all particle-wall collisions and particle-particle collisions being elastic. Under suitable conditions, the ergodicity and strong chaotic properties of such locally confined particle system are rigorously proved in Ref. 4.

Therefore, it is natural to assume that the locally confined particle system has a fast correlation decay, which rationalizes a randomization of energy exchange at the cell-to-cell level. In fact, it is the standard knowledge that chaotic billiard systems like the Lorentz gas have similar statistical properties as random processes.[5,6,25,36] Assume the locally confined particle system is sufficiently chaotic such that its energy exchange exhibits Poissonian statistics. This is to say, at the steady state regime, conditioning on two nearest-neighbor particles carrying energy E_1 and E_2, respectively, when starting from either an energy exchange or the conditional steady state, the time distribution to the next energy exchange has the same exponential tail. The slope of this exponential tail, if exists, is denoted by $R(E_1, E_2)$ (see Section IV for details). In the present paper, we name $R(E_1, E_2)$ the *stochastic energy exchange rate* as in Refs. 13 and 14. With additional assumptions of rules of energy redistributions in energy exchanges, the

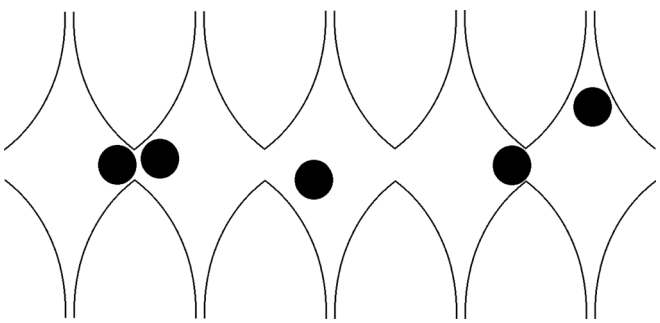

FIG. 1. A locally confined particle system.

[a)]E-mail address: yaoli@cims.nyu.edu.

locally confined particle system can be modified to a stochastic heat conduction model like the KMP (Kipnis-Marchioro-Presutti) model.[24]

Assume the existence of a stochastic energy exchange rate $R(E_1, E_2)$. We say, $R(E_1, E_2) \sim f(E_1, E_2)$ for some function $f(\cdot,\cdot)$, if there exist constants C_1, C_2 independent of E_1 and E_2 such that $C_1 f(E_1, E_2) \le R(E_1, E_2) \le C_2 f(E_1, E_2)$. It was derived non-rigorously in Ref. 14 that when the "bottlenecks" between adjacent cells are sufficiently narrow such that particle-particle collisions are rare, the energy exchange rate $R(E_1, E_2)$ satisfies $R(E_1, E_2) \sim \sqrt{E_1 + E_2}$. See the exact form of $R(E_1, E_2)$ in Section VI and related works in Refs. 13, 15–17. A number of mathematical results on stochastic heat conduction models with or without energy exchange with heat baths are based on the assumption that $R(E_1, E_2) \sim \sqrt{E_1 + E_2}$.[19,29,34,35] For example, the spectral gap of a closed heat conduction model (without heat bath) was investigated in Ref. 19. Many of those theoretical results will not hold if $R(E_1, E_2)$ has other forms like $\sqrt{\min\{E_1, E_2\}}$. At the same time, there are also debates in the physics literature about whether $R(E_1, E_2) \sim \sqrt{E_1 + E_2}$ is universally valid. Some authors argue that very slow particles can play a significant role,[27,28] while others think they can be ignored because a slow particle appears in a sufficiently small probability.[18]

In the present paper, we carefully investigate whether such a stochastic energy exchange rate preserves the main statistical characteristics of the locally confined particle system. One important observation is that, the geometric configuration can qualitatively change main statistical features of the energy exchange rate between consecutive cells. More precisely, when one particle is very slow, whether it can be hit by its neighbors can dramatically change its waiting time distribution for the next particle-particle collision. If a slow particle can always be "activated" by its faster neighbors, then the stochastic energy exchange rate should primarily depend on the kinetic energy of the faster particle. If, otherwise, a slow particle can be out of reach of its neighbors and will have to move to bottleneck areas by itself, then one should expect that the kinetic energy of the slower particle determines the stochastic energy exchange rate at the low energy limit. This observation is confirmed by our studies, as explained in the next paragraph.

A two-particle model is designed to elucidate this observation. It is chosen because (i) it is conceptually the same as the inter-cell dynamics of general locally confined particle models and (ii) it is simple enough to allow accurate numerical simulations. Under the constraint $E_1 + E_2 = 1$, using a combination of numerical simulations and rigorous proof, we show that

(A) If the geometric setting allows one particle to hide from the other, that is, the small particle system, then
- An energy exchange rate $R(E_1, E_2)$ exists. As E_2 decreases, $R(E_1, E_2)$ drops dramatically from $\sim$const to $\sim\sqrt{E_1}$ after a certain threshold (numerical result).
- At the thermal equilibrium, the waiting time distribution for the first particle-particle collision has a polynomial tail at most $\sim t^{-2}$ (rigorous result). In addition, the lower bound $\sim t^{-2}$ is sharp (numerical result).
- The rate of convergence to the equilibrium and the rate of mixing are at most $\sim t^{-2}$ (rigorous result). In addition, the lower bound $\sim t^{-2}$ is sharp (numerical result).

(B) If one particle can always be reached by the other, that is, the big particle system, then
- An energy exchange rate $R(E_1, E_2)$ exists and is strictly positive for all pairs (E_1, E_2) under the constraint $E_1 + E_2 = 1$ (numerical result).
- At the thermal equilibrium, the waiting time distribution for the first particle-particle collision has an exponential tail (numerical result).
- The rate of convergence and rate of mixing are both exponential (numerical result).

We remark that in A, $R(E_1, E_2) \sim \sqrt{\min\{E_1, E_2\}}$ is compatible with the rigorous result about the lower bound of mixing rate. It is easy to check that at the steady state, E_1 and E_2 are uniformly partitioned. Therefore,

$$\mathbb{P}[\text{no energy exchange occurs before } t] \sim t^{-2},$$

which implies that the mixing rate is at most t^{-2}.

A continuous time Markov chain (CTMC) model is then proposed to illustrate our results for the small particle system. When one particle can hide from the other, the energy exchange rate can be approximated by the first passage time to a certain state of the CTMC model. By solving the CTMC model explicitly, we show that there is a threshold $M > 0$ such that $R(E_1, E_2) \sim \sqrt{E_1 + E_2}$ when $\min\{E_1, E_2\} \gg M^{-1}$ and $R(E_1, E_2) \sim \sqrt{\min\{E_1, E_2\}}$ when $\min\{E_1, E_2\} \ll M^{-1}$. This constant M can be roughly seen as the ratio of the whole area to the "bottleneck area" in a confining cell.

Therefore, the validity of estimates $R(E_1, E_2) \sim \sqrt{E_1 + E_2}$ in Ref. 14 depends on many issues. It is reasonable if either the geometric setting completely prevents all particles from hiding from their neighbors; or the effects of low energy particles are negligible. We remark that whether the effects of low energy particles can be neglected depends on the order of taking limits, as will be explained in Section VI. Otherwise, our numerical study suggests $R(E_1, E_2) \sim \sqrt{\min\{E_1, E_2\}}$ as $\min\{E_1, E_2\} \to 0$. In particular, in the studies of asymptotic properties like the rate of mixing, the assumption $R(E_1, E_2) \sim \sqrt{E_1 + E_2}$ does not correctly capture main asymptotic statistical features, such as the decay of correlation, of the original locally confined particle model. No matter how narrow the "bottleneck" is, these properties in the deterministic system can still be very different from the stochastic energy exchange system with a rate function $R(E_1, E_2) \sim \sqrt{E_1 + E_2}$, which may be extremely hard to capture by numerical simulations.

This paper is organized in the following way. A simple locally confined two-particle system is introduced in Section II. Section III investigates the mixing rate, which rigorously disproves the estimate $R(E_1, E_2) \sim \sqrt{E_1 + E_2}$ in Ref. 14 for the small particle system. Our numerical simulations in Section IV then suggest $R(E_1, E_2) \sim \sqrt{\min\{E_1, E_2\}}$ for those settings. A CTMC model is proposed in Section V to further explain our numerical results. A comparison of

our results and the result from Ref. 14 is provided in Section VI. Remarks of numerical simulations are given in Section VII. Section VIII is the conclusion.

II. MODEL DESCRIPTION

In this section, we introduce a simple two-particle system as the model example that can both capture the essential characteristics of the locally confined particle system and facilitate our analysis.

Consider two cells in $\mathbb{R}^2$ that are formed by finite many piecewise C^3 curves and connected by a "bottleneck" opening. Inside each cell is a rigid disk-shaped *moving particle* with mass 2 and radius r. A particle can move freely until it collides with either the cell boundary or the other particle. All collisions are assumed to be elastic. We design the model such that it has the following properties:

(1) Each particle is confined by a cell such that all trajectories of two particles are contained by two disjoint compact sets, respectively.
(2) Particles can collide with each other without passing through the "bottleneck" between cells.
(3) Particles do not rotate.

In addition, we assume that the locally confined particle system is sufficiently chaotic such that each cell forms a strongly chaotic billiard table. More precisely, in the absence of one particle, we assume that the billiard map of the other particle has an exponential correlation decay. We refer Ref. 6 for details of relevant definitions and major results of dynamic billiards.

Therefore, with the given initial locations and initial velocities, moving particles can move, collide, and exchange their kinetic energy. Kinetic energy of particles is denoted by E_1 and E_2, respectively. The total kinetic energy is invariant and assumed to be 1 throughout this paper.

Let $\mathbf{\Omega} = \{(x_1, x_2), (v_1, v_2)\}$ be the state space of the locally confined particle system, where $x_i \in \mathbb{R}^2$ and $v_i \in \mathbb{R}^2$ for $i = 1, 2$ denote the coordinates of particle center positions and particle velocities, respectively. Then, it is clear that the collection of all possible locations of (x_1, x_2) forms a Lebesgue measurable set $\Gamma \subset \mathbb{R}^2 \times \mathbb{R}^2$ and the collection of all possible velocities (v_1, v_2) forms $\mathbb{S}^3$. The collection of all possible locations of x_i is denoted by Γ_i for $i = 1, 2$. Γ_1 and Γ_2 are two disjoint compact subsets of $\mathbb{R}^2$ as assumed. Let

$$\Gamma_1^C = \{x_1 \in \Gamma_1 \,|\, \exists x_2 \in \text{int}(\Gamma_2) \text{ such that } |x_1 - x_2| = 2r\}$$

and define Γ_2^C analogously. A locally confined particle system is called a *big particle system* if $\Gamma_i = \Gamma_i^C$ for $i = 1, 2$ and a *small particle system* if $\text{int}(\Gamma_i \backslash \Gamma_i^C) \neq \emptyset$ for $i = 1, 2$. The main difference is that two particles can always collide with each other in the big particle system, while a static particle can be out of reach of the other particle in the small particle system.

We fix also the following notations. Let $\Phi_t : \mathbf{\Omega} \to \mathbf{\Omega}$ be the billiard flow and $P^t : \mathbf{\Omega} \times \mathcal{B}(\mathbf{\Omega}) \to [0, 1]$ be the transition kernel of Φ_t, where $\mathcal{B}(\mathbf{\Omega})$ represents the Borel algebra on $\mathbf{\Omega}$. It is well known that Φ_t admits a Liouville measure $\pi := c\lambda_4|_\Gamma \times u|_{\mathbb{S}^3}$ as its invariant probability measure, where $\lambda_n|_A$ is the restricted Lebesgue measure on $A \subset \mathbb{R}^n$, $u|_{\mathbb{S}^3}$ is the surface area on $\mathbb{S}^3$, and c is a constant that is determined by the geometry of the model. π is also the thermal equilibrium.

The model example described in Figure 2 will be used to illustrate our numerical results. We remark that we also worked with other examples of the same type. This example is chosen for the demonstration because (i) each cell forms a strongly chaotic billiard table as all orbits have frequent collisions with the dispersing parts of the boundary, that is, the circles; (ii) the placement of disks allows us to have big particle systems and small particle systems with minimal changes, and (iii) the relatively simple geometry simplifies numerical simulations.

The model example is a locally confined particle system on $\mathbb{R}^2$ that consists of eight circles with radius 1, two line segments, and two moving particles. The coordinates of centers of the circles are (0, 2), (2.5, 2), (3.5, 0), (2.5, −2), (0, −2), (−2.5, −2), (−3.5, 0), and (−2.5, 2). The coordinates of ends of two line segments are $\{(0, 1), (0, a)\}$ and $\{(0, -1), (0, -a)\}$, respectively, where $\frac{1}{4} < a < 1$ is a parameter. Both moving particles have radii $(a + \epsilon)$, where $0 < \epsilon \ll 1$, so that they are trapped by the cells.

For illustration, we study one big particle system with $a = 0.99$, $\epsilon = 0.01$ and one small particle system with $a = 0.35$, $\epsilon = 0.001$ in our numerical simulations.

III. RATE OF CONVERGENCE AND MIXING

Rates of convergence to equilibrium and mixing are the most important statistical characteristics of a deterministic dynamical system, which are supposed to be preserved by any stochastic approximations. In this section, we will show that the small particle system has a polynomial rate of mixing/convergence, while the big particle system has an exponential rate of mixing/convergence.

For $\delta > 0$, define

$$S_0^i(\delta) = \{x \in \Gamma_i \,|\, \text{dist}(x, \partial(\Gamma_i \backslash \Gamma_i^C)) \geq \delta\}$$

for $i = 1, 2$ and

$$S_t^i(\delta) = \left\{\mathbf{x} \in \mathbf{\Omega} \,|\, x_i \in S_0^i, |v_i| \leq \frac{\delta}{t}\right\}$$

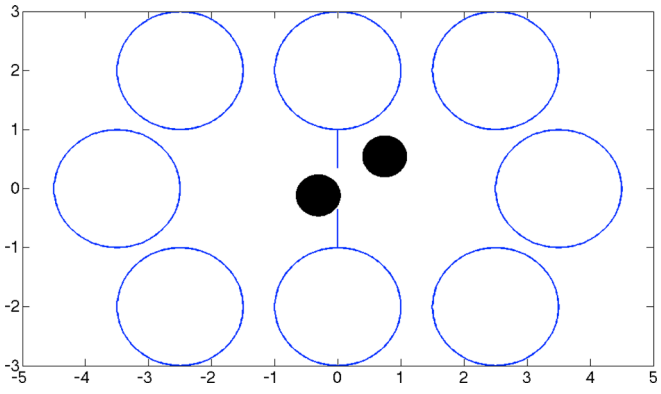

FIG. 2. A 2-particle system model example: $a = 0.35$, $\epsilon = 0.351$.

and $S_t(\delta) = S_t^1(\delta) \cup S_t^2(\delta)$. By the definition of the small particle system, there exists a $\delta > 0$ such that $S_0^i(\delta)$ are well defined for $i = 1, 2$. Hence, we drop the notation δ from now on for the sake of simplicity.

The following result is about the rate of convergence, in which μP^t indicates the push-forward measure of μ by Φ_t.

Lemma 3.1. *In any given small particle system, for any probability measure $\lambda \ll \pi$ such that $\mathrm{d}\lambda \geq (1+c)\mathrm{d}\pi$ on S_{t_0} for some constants $c > 0$ and $t_0 > 0$, there exists $C_0 > 0$ such that*

$$\|\lambda P^t - \pi\|_{TV} \geq \frac{C_0}{t^2}$$

for all $t > t_0$. In particular, the mixing rate of Φ_t is at most polynomial, that is, there exists a Borel set $A \subset \mathbf{\Omega}$ such that

$$C_A(t) := \sup_{B \in \mathcal{B}(\mathbf{\Omega})} \left| \int_A P^t(x, B)\pi(\mathrm{d}x) - \pi(A)\pi(B) \right| \geq \pi(A) \cdot \frac{C_0}{t^2}$$

for all $t > t_0$.

Proof. The proof uses the idea in Refs. 39 and 37. By the definition of B_t, there exist constants t_0 and C_1 such that

$$\pi(S_t) = \frac{C_1}{t^2}$$

for any $t \geq t_0$. Let $a > (1-(1+c)^{-1/2})^{-1}$ be a constant. We have

$$\begin{aligned} \|\lambda P^t - \pi\|_{TV} &\geq \lambda P^t(S_{at}) - \pi(S_{at}) \\ &\geq (1+c)\pi(S_{at+t}) - \pi(S_{at}) \\ &= (1+c) \cdot \left[\frac{a^2}{(a+1)^2} - 1 \right] \cdot \frac{C_1}{a^2} \cdot t^{-2} \\ &=: C_0 t^{-2} . \end{aligned}$$

The bound of the mixing rate follows easily by letting $A = S_{t_0}$. Let λ be the probability measure such that

$$\mathrm{d}\lambda = \frac{1}{\pi(A)} 1_A \mathrm{d}\pi .$$

Then,

$$\begin{aligned} &\frac{1}{\pi(A)} \sup_{B \in \mathcal{B}(\mathbf{\Omega})} \left| \int_A P^t(x, B)\pi(\mathrm{d}x) - \pi(A)\pi(B) \right| \\ &\quad = \|\lambda P^t - \pi\|_{TV} \geq \frac{C_0}{t^2} . \end{aligned}$$

□

Although a sharp upper bound of $\|\lambda P^t - \pi\|_{TV}$ is beyond the reach of rigorous proof, our numerical results show that the rate of mixing of the small particle system is $\sim t^{-2}$.

We remark that for the small particle system, the exact rate of mixing is difficult to compute numerically. Let

$$C_{A,B}(t) := \left| \int_A P^t(x, B)\pi(\mathrm{d}x) - \pi(A)\pi(B) \right| .$$

Clearly $C_{A,B}(t)$ is the difference of two relatively large numbers. As a result, when the value of $C_{A,B}(t)$ is $o(t^{-2})$, the variance is still around a constant number. Therefore, to control the relative error of $C_{A,B}(t)$ to be less than ϵ, the sample size of the Monte Carlo simulation must be at least $O(t^4\epsilon^{-2})$. This makes the total computational cost $O(t^5\epsilon^{-2})$. In addition, the rate of mixing captures the shape of the tail of $C_{A,B}(t)$. To observe a polynomial rate of mixing, a very large t is required. In fact, as shown in Figure 3(a), t should be $\sim 10^5$ in order to clearly observe the polynomial tail. This brings the total computational cost to $\sim 10^{27}$ (assume $\epsilon = 0.1$).

Instead of direct computation, the rate of mixing t^{-2} is supported by the following numerical evidence. Consider two sets $A, B \subset \mathbf{\Omega}$ where the kinetic energy of particle 2 in A is significantly smaller than that in B. One approach to estimate $C_{A,B}(t)$ is to compute the distribution of the first passage time from A to B. The assumption behind this approach is that once particle 2 obtains a certain amount of energy, the correlation decays fast enough such that it "forgets" its history.

Let

$$\begin{aligned} A = \{(x_1, x_2, v_1, v_2) \in \mathbf{\Omega} \,|\quad & x_1 \in [1, 1.5] \times [-0.25, 0.25]; \\ & x_2 \in [-1.5, 1] \times [-0.25, 0.25]; |v_2|^2 < 0.01\} \end{aligned}$$

and

$$B = \{(x_1, x_2, v_1, v_2) \in \mathbf{\Omega} \,|\, |v_2|^2 \geq 0.4\} .$$

Let Φ_0 be uniformly distributed on A. The tail of the first passage time distribution to B is demonstrated in Figure 3(a) and compared with t^{-2}, from which one can see the first passage time distribution to B has the tail $\sim t^{-2}$. Therefore, we believe the small particle system has the rate of mixing $\sim t^{-2}$.

In contrast, in a big particle system, the slow particle can be "activated" by the fast particle almost surely. Hence, an exponential mixing rate is expected due to the strong chaos. This exponential rate of mixing is supported by numerical evidence too. We first choose sets A and B same as above to estimate the tail of the first passage time distribution to B. As seen in Figure 3(b), the first passage time distribution to B has an exponential tail. In addition, due to much more frequent particle−particle collisions, computing the correlation function of the big particle system becomes possible. Let $A_0 = \{x_1 \in [1, 1.5] \times [-0.25, 0.25]; x_2 \in [-1.5, 1] \times [-0.25, 0.25]; |v_2|^2 < 0.1\}$ and $B_0 = \{0.4 \leq |v_2| \leq 0.6\}$. The correlation function $C_{A_0,B_0}(t)$ is numerically computed up to $t \approx 40$ in Figure 4, in which an exponential decay of $C_{A_0,B_0}(t)$ is observed.

It is worth mentioning that to accurately capture the tail distribution of quantities like the first passage time and the correlation function, trajectories should be run for sufficiently long time. As we can see, the initial slopes of curves in Figure 3, later in Figures 6 and 7, and possibly in Figure 4, are deeper than their tail slopes. One possible explanation is that due to their slow motion, effects of low energy particles are not significant over a small time period.

Remark 3.2. As one of the most important statistical property, the rate of mixing and rate of convergence must be preserved by any stochastic approximations of the deterministic model. Therefore, our result disproves the estimate $R(E_1, E_2) \sim \sqrt{E_1 + E_2}$ in Ref. 14 for the small particle

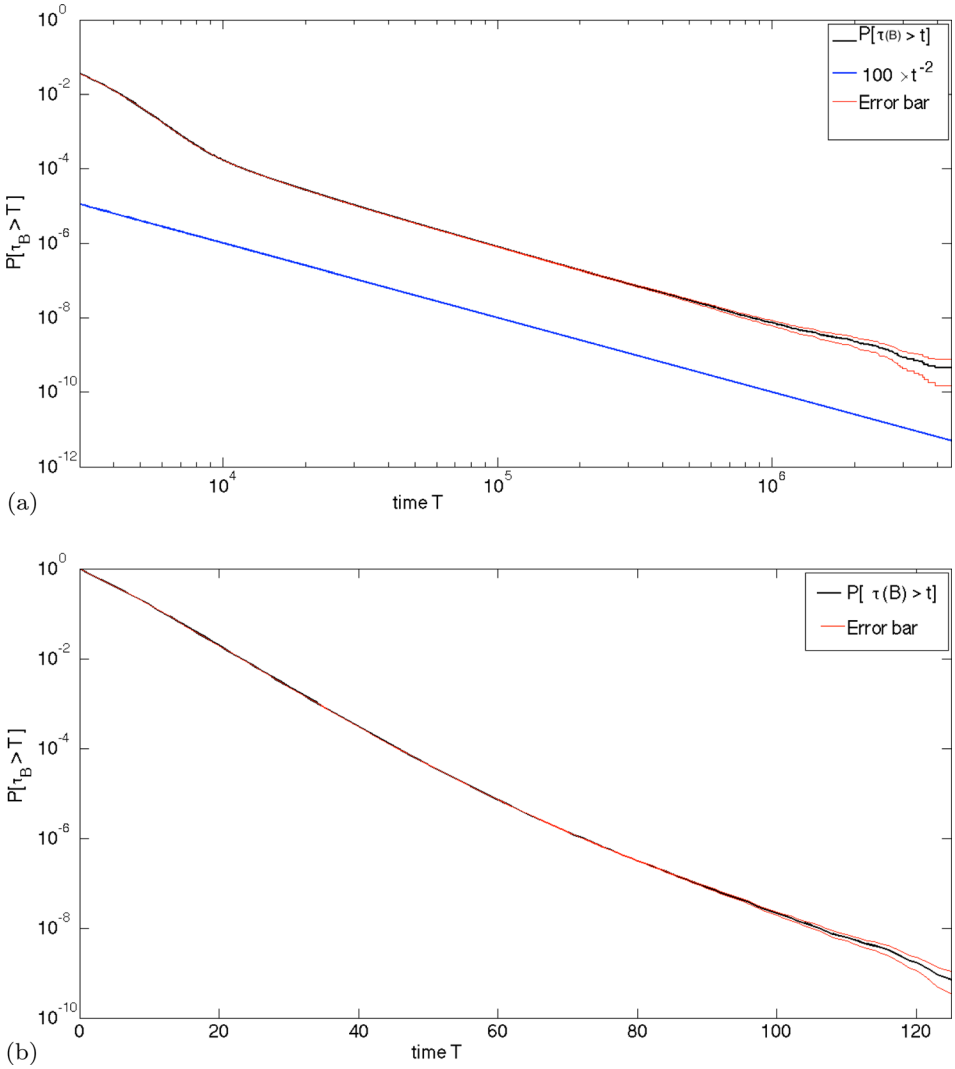

FIG. 3. Black: Tail of the first passage time distribution from A to B; red: Two standard deviation error bars; blue in (a): Reference plot of $100 \times t^{-2}$.

system. The reason is that, assume $E_1 + E_2 = 1$, $R(E_1, E_2) \sim$ const. If the energy redistribution satisfies

$$(E_1', E_2') = (p(E_1 + E_2), (1-p)(E_1 + E_2))$$

for some random variable p that has a uniformly positive density on (0, 1), then the Markov chain generated by this stochastic model satisfies the Doeblin's condition, which implies an exponential mixing rate and an exponential convergence rate to its invariant probability measure. This cannot happen for the small particle system because of Lemma 1. Instead, our simulations in Section IV suggest $R(E_1, E_2) \sim \sqrt{\min\{E_1, E_2\}}$ for the small particle system.

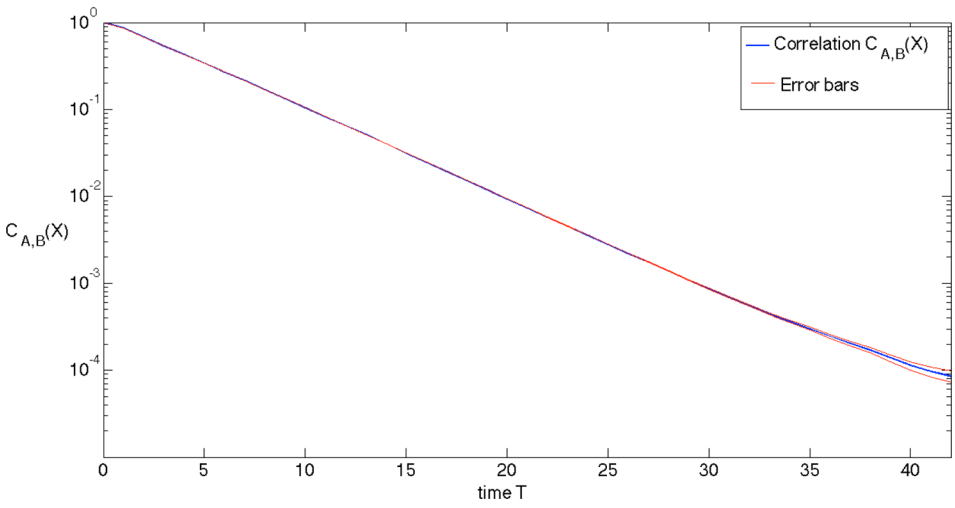

FIG. 4. Blue: Correlation function $C_{A,B}(t)$; red: Two standard deviation error bars. $C_{A,B}(t)$ is normalized such that $C_{A,B}(0) = 1$.

IV. RATES OF ENERGY EXCHANGE

A. Definition of stochastic energy exchange rate

The purpose of this subsection is to define the stochastic energy exchange rate $R(E_1, E_2)$ for the locally confined particle system.

For a Poisson process, it is well known that the time interval between jumps and the waiting time to the next jump from any $t>0$ satisfy the same exponential distribution, whose rate is the rate of this Poisson process. Since a locally confined particle system generates an ergodic deterministic process with quick correlation decay, it is natural to expect it to exhibit similar Poissonian statistics. At the steady-state regime, since particle-particle collisions form a subset in the phase space $\mathbf{\Omega}$, the time to the next particle-particle collision is called the *hitting time* and the time duration between two consecutive particle-particle collisions is called the *return time*. The times of energy exchanges of the locally confined particle system resemble a Poisson process if and only if conditioning on fixed energy configurations, the tail distribution of the hitting time, and that of the return time coincide. A stochastic energy exchange rate can therefore be defined from the slope of this exponential tail.

Let

$$\tau_B = \inf\{t>0 | \text{a particle–particle collision occurs at time } t\}.$$

A function $R(E_1, E_2)$ is called the *stochastic energy exchange rate* if

$$\begin{aligned} R(E_1,E_2) &= \lim_{t\to\infty} -\frac{1}{t}\log\left(\mathbb{P}\left[\tau_B > t \,|\, \pi, |v_1|^2 = E_1, |v_2|^2 = E_2\right]\right) \\ &= \lim_{t\to\infty} -\frac{1}{t}\log \mathbb{P}[\tau_B > t \,|\, \pi, |v_1(0^+)|^2 \\ &= E_1, |v_2(0^+)|^2 = E_2 \\ &\quad x_1 \in \text{int}(\Gamma_1), x_2 \in \text{int}(\Gamma_2), |x_1 - x_2| = 2r]. \end{aligned}$$

The first limit gives the tail distribution of the conditional hitting time when starting from the conditional Liouville measure, on which particle energy is E_1 and E_2, respectively. The second limit gives the tail distribution of the conditional return time when starting from the conditional Liouville measure, on which two particles collide at $t=0$, and particle energy after the collision is E_1 and E_2, respectively.

Since

$$\tau_B\,|_{\Phi_0=(x_1,x_2,\alpha v_1,\alpha v_2)} = \alpha^{-1}\tau_B\,|_{\Phi_0=(x_1,x_2,v_1,v_2)},$$

we have $R(\alpha E_1, \alpha E_2) = \alpha^{1/2} R(E_1, E_2)$. Therefore, the assumption $E_1 + E_2 = 1$ does not lose generality.

Remark 4.1. For ergodic dynamical systems, the relation between the return time and the hitting time to asymptotically small set is well-known.[20] It is also known that in many highly chaotic dynamical systems, the return time distribution and the hitting time distribution to asymptotically small set coincide.[21–23,31] There are also examples where the hitting time distribution differs from the return time distribution.[10,11] To be best of the author's knowledge, it is very difficult to directly apply these existing results to our cases, that is, tail distributions of the conditional hitting/return time. Instead, we will verify numerically that these two tails coincide, which implies a well defined stochastic energy exchange rate.

B. Non-exponential tails

We first rigorously show that for some initial distributions, the hitting time distribution of the small particle system cannot have an exponential tail, which further disproves the estimate $R(E_1, E_2) \sim \sqrt{E_1 + E_2}$.

Let ν be a probability measure on $\mathbf{\Omega}$ such that $\nu = c\lambda_4|_\Gamma \times \hat{\nu}$, where c is a constant and $\hat{\nu}$ is a probability measure on $\mathcal{B}(\mathbb{S}^3)$. We say, $\Phi_0 = \nu$, if ν is the probability distribution of Φ_0.

Lemma 4.2. *For any given small particle system, there exist constants $h_1, h_2 > 0$ such that*

$$\mathbb{P}[\tau_B > t \,|\, \Phi_0 = \nu] \geq h_1 \hat{\nu}(\{|v_1| < h_2 t^{-1}\})$$

for any $t>0$.

Proof. By the assumption of the small particle system, there exists a set $C_1 \subset \Gamma_1$ with positive Lebesgue measure and a constant $h_2 > 0$, such that the Hausdorff distance between C_1 and Γ_1^C is greater than h_2.

Therefore, if $x_1 \in C_1$ at $t=0$, τ is at least $\frac{h_2}{|v_1|}$. The proof is completed by letting $h_1 = cu_\Gamma(\{(x_1,x_2) \,|\, x_1 \in C_1\}) = cu_\Gamma(C_1 \times \Gamma_2) > 0$. □

An analogous result holds for particle 2.

Therefore, $\mathbb{P}[\tau_B > t]$ has an at-most-polynomial tail for some initial distribution ν.

Corollary 4.3. *There exists a constant h_0 such that*

$$\mathbb{P}[\tau_B > t \,|\, \Phi_0 = \pi] \geq h_0 t^{-2}$$

for every $t \geq 1$.

Proof. It is well known that given $X = (X_1, \ldots, X_n)$, where X_i are i.i.d. standard normal random variables, the random vector $\frac{X}{|X|}$ is uniformly distributed on $\mathbb{S}^{n-1}$. Then, it is easy to check that E_1 is uniformly distributed on (0, 1) and $E_2 = 1 - E_1$.

The corollary then follows easily from the fact that

$$u|_{\mathbb{S}^3}(\{|v_1| < \sqrt{\epsilon}\}) = \epsilon$$

for every $0 < \epsilon < 1$, where $u|_{\mathbb{S}^3}$ is the uniform distribution on $\mathbb{S}^3$ as introduced in Section II. □

At the steady state regime, the hitting time distribution of the small particle system has an at-most-polynomial tail instead of an exponential one. In addition, E_1 (and E_2) is uniformly distributed at the steady state. Therefore (if $R(E_1, E_2)$ is well-defined), the estimate $R(E_1, E_2) \sim \sqrt{E_1 + E_2}$ cannot hold for every pair (E_1, E_2).

Since in a small particle system, the particle with low energy can hide from the other one for a very long time, we expect that $R(E_1, E_2)$ mainly depends on $\min\{E_1, E_2\}$ as $\min\{E_1, E_2\} \to 0$. This is supported by our numerical simulations subsection IV C.

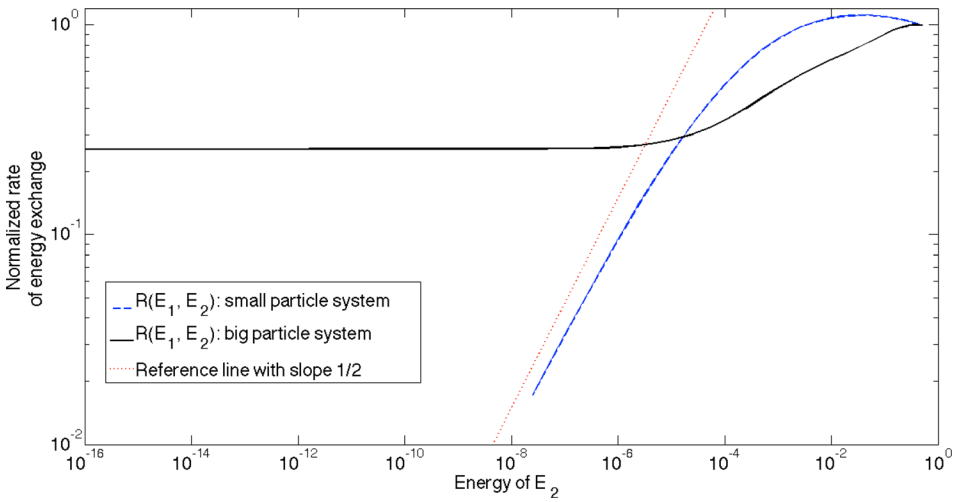

FIG. 5. Computed value of $R(E_1, E_2)$. x-axis: E_2. Red dotted line: Reference line with slope 1/2; black solid line: $R(E_1, E_2)$ for big particle system; blue dashed line: $R(E_1, E_2)$ for small particle system. All three plots are normalized such that $R(0.5, 0.5) = 1$. $R(1 - 10^{-15}, 10^{-15})$ on the log-log plot are obtained from calculating $R(1, 0)$.

C. Stochastic energy exchange rate

In this subsection, we will compute the tail distribution of the conditional hitting time by Monte Carlo simulations. Then, we will compare it and the tail distribution of the conditional return time, which numerically verifies whether $R(E_1, E_2)$ is well defined. Overall, our numerical simulations suggest $R(E_1, E_2) \sim \sqrt{E_1 + E_2}$ for the big particle system and $R(E_1, E_2) \sim \sqrt{\min\{E_1, E_2\}}$ for the small particle system.

1. $R(E_1, E_2)$ from conditional hitting time

In Figure 5, we computed the conditional hitting time of the big/small particle systems at different energy configurations in the following way. Let $\Phi_0 = \lambda_4|_\Gamma \times \delta(|v_1| - E_1)$. A large number of sample paths are simulated to obtain $\mathbb{P}[\tau_B \geq t]$ for different t. The conditional hitting time, or $R(E_1, E_2)$, is estimated as the slope of $\mathbb{P}[\tau_B \geq t]$ in the log-linear plot. The rate $R(E_1, E_2)$ of the small particle system and that of the big particle system are measured for 28 and 29 distinct pairs of (E_1, E_2), respectively ($(E_1, E_2) = (1, 0)$ can only be measured for the big particle system). See details of numerical simulations in Section VII.

We are interested in the scaling of $R(E_1, E_2)$ as $E_2 \to 0$. From our numerical simulation results, $R(1, 0)/R(0.5, 0.5) \approx 0.25$ for the big particle system. Therefore, it is safe to say, $R(E_1, E_2) \sim \sqrt{E_1 + E_2}$. However, $R(E_1, E_2)$ of the small particle system has a completely different scaling as $E_2 \to 0$. For the small particle system, we have $R(E_2, 1 - E_2) \approx \text{const} \cdot \sqrt{E_2}$ with $E_2 \ll 1$, as seen in Figure 5.

Furthermore, when the initial distribution is taken to be π, numerical simulations show that

$$\mathbb{P}[\tau_B \geq t \,|\, \pi] \sim t^{-2}$$

for the small particle system (Figure 6), which suggests that the lower bound in Corollary 4.3 is sharp. In contrast, in the big particle system, $\mathbb{P}[\tau_B \geq t \,|\, \pi]$ has an exponential tail (Figure 7).

2. Tail distributions of hitting time and return time

We then compare tail distributions of the conditional hitting time and that of the conditional return time. If the two tails coincide, at least numerically, we see a well defined stochastic energy exchange rate.

Let $\{(E_1^{(1)}, E_2^{(1)}, t^{(1)}), \ldots, (E_1^{(N)}, E_2^{(N)}, t^{(N)})\}$ be a set of samples obtained from a single trajectory starting from $\mathbf{x}_0$, where the triplet $(E_1^{(i)}, E_2^{(i)}, t^{(i)})$ means the duration between the $(i-1)$-th and the i-th particle-particle collisions is $t^{(i)}$ and the corresponding particle energy is $(E_1^{(i)}, E_2^{(i)})$. Due to the

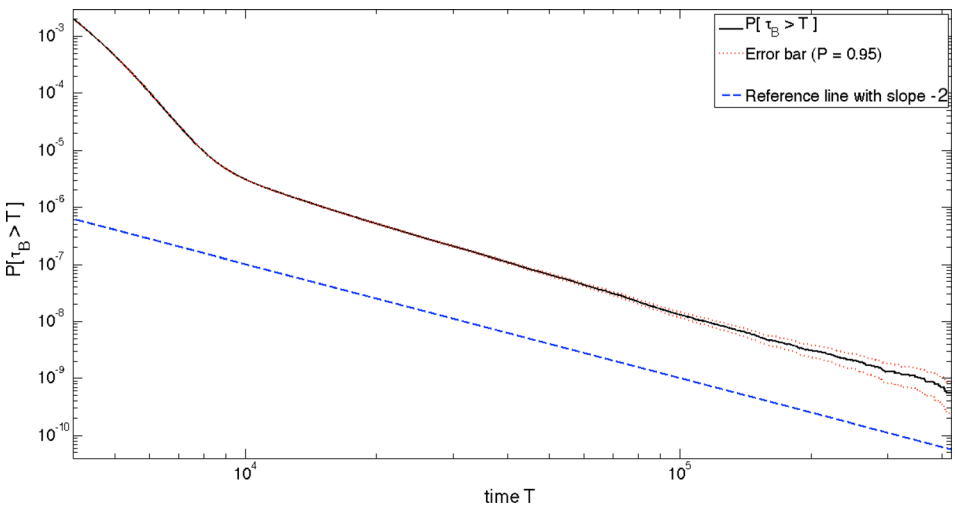

FIG. 6. Small particle system. Black solid line: Tail distribution of $\mathbb{P}[\tau_B > t]$; red dotted line: Two standard deviation error bars; blue dashed line: Reference plot of t^{-2}.

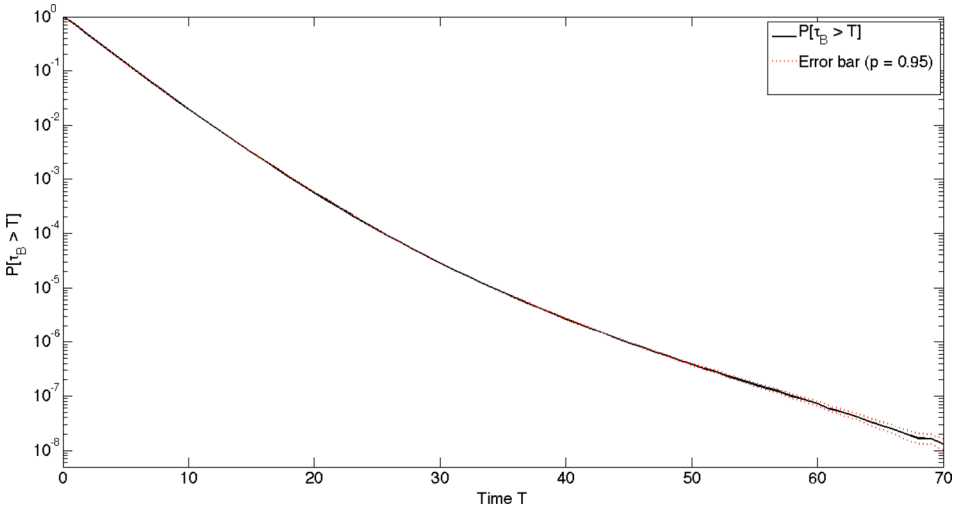

FIG. 7. Big particle system. Black solid line: Tail distribution of $\mathbb{P}[\tau_B > t]$; red dotted line: Two standard deviation error bars.

ergodicity of the system, a joint probability density function of the conditional return time and the particle energy $\rho_{\mathbf{x}_0}(E_1, E_2, t)$ can be constructed from these samples as $N \to \infty$. If the slope of the tail distribution of the conditional return time is still $R(E_1, E_2)$, we expect to see

$$\lim_{t\to\infty} \frac{1}{t} \log\left(\int_t^\infty \rho_{\mathbf{x}_0}(E_1, E_2, s)|_{(E_1,E_2)} \mathrm{d}s\right) = R(E_1, E_2)$$

for a.e. $\mathbf{x}_0$

for the $R(E_1, E_2)$ we have just computed. This can be verified by the following two numerical simulations:

(1) Numerical simulation 1: If the tail distribution of the conditional return time has the same slope $R(E_1, E_2)$ as the conditional hitting time, then the rescaled return time distribution

$$\Lambda(t) := \int_t^\infty \int_0^1 \rho_{\mathbf{x}_0}(E, 1-E, s) R(E, 1-E) \mathrm{d}E \mathrm{d}s \qquad (4.1)$$

should have an exponential tail e^{-t}. $\Lambda(t)$ can be calculated from the sample $\{t^{(i)} R(E_1^{(i)}, E_2^{(i)})\}_{i=1}^N$ with relatively high accuracy

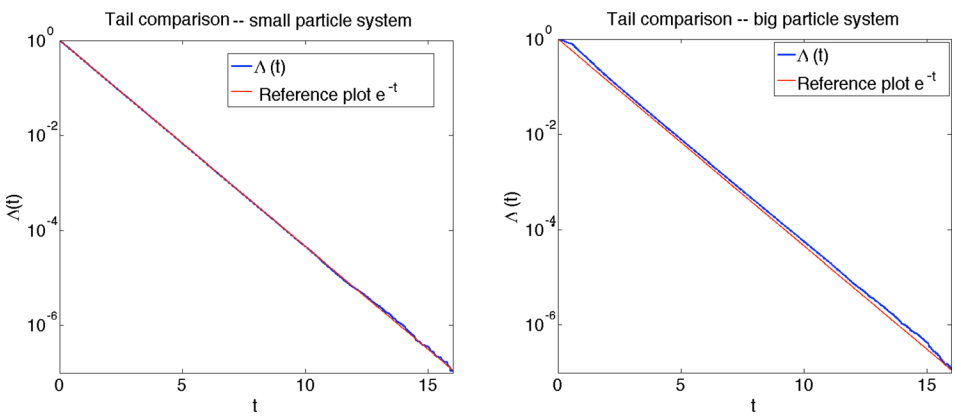

FIG. 8. Distribution of $\Lambda(t)$ for the small/big particle system.

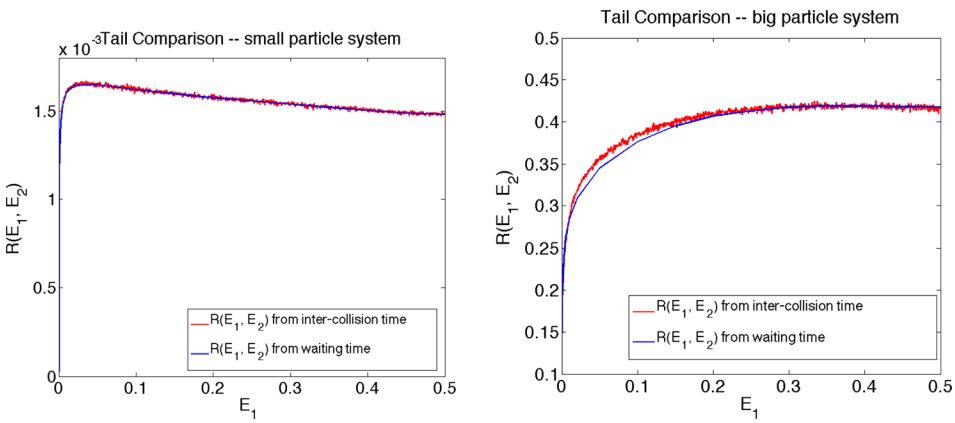

FIG. 9. $R(E_1, E_2)$ obtained from two different methods.

$$\Lambda(t) \approx \frac{1}{N}\left|\left\{t^{(i)} R\left(E_1^{(i)}, E_2^{(i)}\right) > t\right\}\right|.$$

In Figure 8, one can find that $\Lambda(t)$ and e^{-t} are almost parallel in the log-linear plot.

(2) Numerical simulation 2: For any given (E_1, E_2), the conditional return time distribution $\rho_{\mathbf{x}_0}(E_1, E_2, t)|_{(E_1,E_2)}$ can be approximated by only selecting samples

$$\{(E_1^{(k_1)}, E_2^{(k_1)}, t^{(k_1)}), \ldots, (E_1^{(k_M)}, E_2^{(k_M)}, t^{(k_M)})\}$$

such that $E_1^{(k_i)} \in (E_1 - \epsilon, E_1 + \epsilon)$, $i = 1 \sim M$ for some sufficiently small $\epsilon > 0$. The tail distribution of the conditional return time can then be computed. Since $\epsilon \ll 1$, the sample size for each (E_1, E_2) is relatively small. As seen in Figure 9, the tail distribution of the conditional return time has visible numerical errors.

Tail distributions of the conditional hitting/return time are compared in Figure 9 for the small particle system (left) and the big particle system (right). In spite of numerical errors, two tails match each other well.

From the above two numerical simulations, especially the first one, we conclude that the conditional return time and the conditional hitting time have the same tail distribution. This means statistically, times of energy exchanges of the locally confined particle system resemble a (non-homogeneous) Poisson process. Therefore, the stochastic energy exchange rate $R(E_1, E_2)$ for this deterministic system is well-defined.

V. CTMC MODEL OF SMALL PARTICLE SYSTEMS

In this section, we propose a CTMC approximate model to explain why $R(E_1, E_2) \sim \sqrt{\min\{E_1, E_2\}}$ as $\min\{E_1, E_2\} \to 0$ in the small particle system.

The main assumption of the CTMC model is that the locally confined particle system is so chaotic that particles lose their memory of precise locations quickly. Therefore, we take note of whether a particle is available for energy exchange instead of its precise location. This converts the locally confined particle system to a finite state Markov jump process. For each particle, the time to its next jump is determined by an exponential distribution with mean $\propto x^{-1/2}$, where x is the instantaneous kinetic energy of the particle.

Formally, our CTMC model is a four-state continuous time Markov chain Ψ_t on the state space $\{0, 1\}^2$. State 0 means a particle is not available for energy exchange; state 1 means it is available for energy exchange. When Ψ_t reaches (1, 1), particles exchange energy immediately and return to (0, 0). The locally confined particle system is assumed to be symmetric. Transition rates of Ψ_t are demonstrated in Figure 10, where r_1 and r_2 are two constants that depend on the geometry of the model. When the "bottleneck" in the locally confined particle system is narrow, the ratio $M := r_2/r_1$ is a large number in general. In particular, $M > \lambda_2(\Gamma_1 \backslash \Gamma_1^C)/\lambda_2(\Gamma_1^C)$ (which is ≈ 11 for our small particle system model example) because an event $\{x_1 \in \Gamma_1^C, x_2 \in \Gamma_2^C\}$ does not guarantee a particle-particle collision.

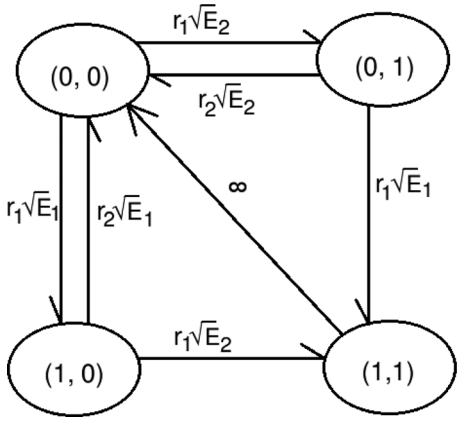

FIG. 10. A graph representation of CTMC model for a locally confined particle system.

This is not a very precise model because in the deterministic system, particles are still available for energy exchange for a short time period after a particle-particle collision. In addition, it is difficult to explicitly evaluate r_1 and r_2 merely from the geometric parameters. However, many qualitative asymptotical properties of the locally confined particle system can be captured by this CTMC approximation. In particular, the hitting time τ_B is approximated by

$$\tau_{1,1} = \inf_{t>0}\{\Psi_t = (1, 1)\},$$

the first passage time to the state (1, 1). Since the transition rate from (1, 1) to (0, 0) is infinity, $\tau_{(1,1)}|_{\Psi_0=(0,0)}$ also gives the return time distribution.

From the infinitesimal generator of Ψ_t, we have $\mathbb{P}[\tau_{1,1} \le t \,|\, \Psi_0 = (0,0)] = p_{14}(t)$, where $P(t) = \{p_{ij}(t)\}_{i,j=1}^4 = \exp(At)$, and

$$A = \begin{bmatrix} -r_1\sqrt{E_1} - r_1\sqrt{E_2} & r_1\sqrt{E_2} & r_1\sqrt{E_1} & 0 \\ r_2\sqrt{E_2} & -r_2\sqrt{E_2} - r_1\sqrt{E_1} & 0 & r_1\sqrt{E_1} \\ r_2\sqrt{E_2} & 0 & -r_2\sqrt{E_1} - r_1\sqrt{E_2} & r_1\sqrt{E_1} \\ 0 & 0 & 0 & 0 \end{bmatrix}.$$

Therefore, $R(E_1, E_2)$ can be approximated by $-\rho_2$, where ρ_2 is the greatest nonzero eigenvalue of A. As $\min\{E_1, E_2\} \to 0$, the scaling of ρ_2 can be estimated analytically.

Let $A = r_1 B$, where

$$B = \begin{pmatrix} -\sqrt{E_1} - \sqrt{E_2} & \sqrt{E_2} & \sqrt{E_1} & 0 \\ M\sqrt{E_2} & -\sqrt{E_2}M - \sqrt{E_1} & 0 & \sqrt{E_1} \\ M\sqrt{E_1} & 0 & -\sqrt{E_1}M - \sqrt{E_2} & \sqrt{E_2} \\ 0 & 0 & 0 & 0 \end{pmatrix}. \tag{5.1}$$

The characteristic equation $p(\lambda)$ of B is

$$\begin{aligned} p(\lambda) = {} & (E_1 + \sqrt{E_2})\sqrt{E_1}\sqrt{E_2}(M+1)\lambda \\ & + (\sqrt{E_1}\sqrt{E_2}(M^2 + 2M + 3) + E_1(M+1) \\ & + E_2(M+1))\lambda^2 + (\sqrt{E_1} + \sqrt{E_2})(M+2)\lambda^3 + \lambda^4. \end{aligned} \tag{5.2}$$

Therefore, it is easy to verify that $p(0) = 0$, $p'(0) > 0$, $p(-\sqrt{E_1}) = M^2 E_1^{3/2}\sqrt{E_2} > 0$, and $p(-\sqrt{E_2}) = M^2 E_2^{3/2}\sqrt{E_1} > 0$. Hence, $-\rho_2 < r_1 \min\{\sqrt{E_1}, \sqrt{E_2}\}$. This confirms our numerical observation: $R(E_1, E_2) \sim \sqrt{\min\{E_1, E_2\}}$ as $\min\{E_1, E_2\} \to 0$.

We compare $-\rho_2$ and $R(E_1, E_2)$ for different pairs of (E_1, E_2). When the "bottleneck" area is narrow, it is reasonable to assume that $r_1 \sim M^{-1}$. We choose $r_1 = 1/10$ and $r_2 = 2$ and compare $-\rho_2$ and $R(E_1, E_2)$ in Figure 11. We can find that $-\rho_2$ and $R(E_1, E_2)$ have similar scaling as $\min\{E_1, E_2\} \to 0$.

VI. COMPARISON WITH RESULTS FROM REFERENCE 14

The stochastic energy exchange rate of a class of locally confined particle systems is investigated in Ref. 14. Their main assumption is that particle-wall collisions happen significantly more frequently than particle-particle collisions. The authors then implicitly assumed local systems of two adjacent cells attain their local equilibria no later than the first particle-particle collision between them. The following stochastic rate function is derived:

$$\hat{R}(E_1, E_2) = \text{const} \cdot \sqrt{\frac{8E_2}{\pi^3}}\left[2\mathcal{E}\left(\frac{E_1}{E_2}\right) - \left(1 - \frac{E_1}{E_2}\right)\mathcal{K}\left(\frac{E_1}{E_2}\right)\right] \tag{6.1}$$

for every $E_2 \geq E_1$, where $\mathcal{K}(x)$ and $\mathcal{E}(x)$ are the Jacobi elliptic functions of the first and the second kind, respectively. $\hat{R}$ is symmetric in the sense $\hat{R}(E_1, E_2) = \hat{R}(E_2, E_1)$, if $E_2 < E_1$. Then, it is easy to check that $\hat{R}(E_1, E_2) \sim \sqrt{E_1 + E_2}$.

If $\hat{R}(E_1, E_2) \sim \sqrt{E_1 + E_2}$ is universally true, then all locally confined particle systems should have exponential mixing rates and exponential convergence rates to equilibria regardless of geometric configurations. This contradicts our rigorous results and numerical evidence. In fact, $\hat{R}(E_1, E_2)$ of the small particle system is only reasonable if neither E_1 nor E_2 is extremely small. As seen in Figure 12, the prediction from (6.1) is good until a "turning point." We remark that in our numerical simulations of the small particle system, particle-wall collisions are about 700 times more frequent than particle-particle collisions, which can be seen as dynamics in two time scales.

The gap between (6.1) and our results can be explained by a similar CTMC model. In Ref. 14, to obtain (6.1), the authors implicitly assume that in each pair of adjacent cells, a local equilibrium is reached before the next particle-particle collision between them. Hence, the waiting time for the next particle-particle collision is in proportion to the Lebesgue measure of the set at which particles are in contact. This implicit assumption implies that $R(E_1, E_2)$ should be approximated by the steady state probability of the state (1, 1) in the CTMC model described in Figure 13, denoted by $p_{1,1}$. Therefore, it is necessary to compare $p_{1,1}$ and $-\rho_2$.

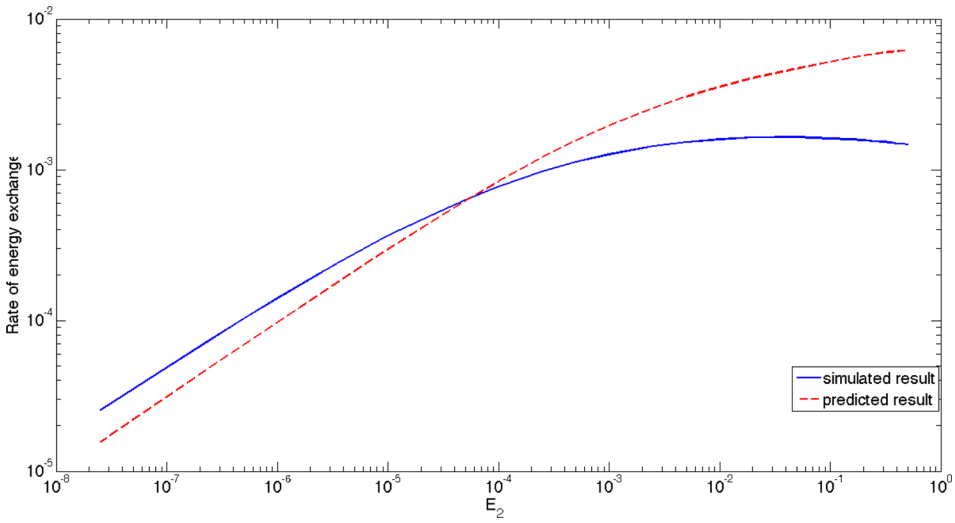

FIG. 11. x-axis: E_2; blue solid line: Energy exchange rate from numerical simulations; red dashed line: Energy exchange rate predicted by CTMC model with parameter $r_1 = 0.1$ and $r_2 = 2$.

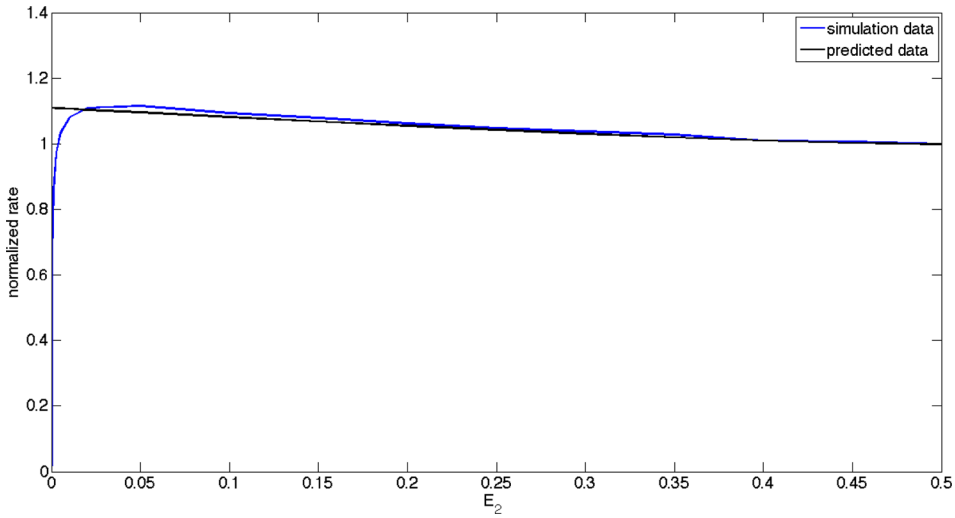

FIG. 12. x-axis: E_2; blue: Rates of energy exchange from numerical simulations; black: Rates of energy exchange predicted by Eq. 6.1. All plots are normalized such that $R(0.5, 0.5) = 1$.

When the "bottleneck" is sufficiently narrow, it is reasonable to assume $r_1 \sim M^{-1}$. Hence, $p_{1,1} \sim M^{-2}$. As a comparison, we have the following calculation of the CTMC model in Section V:

For every $M > 2$,

$$p\left(-\frac{\sqrt{E_1}+\sqrt{E_2}}{M}\right) = \frac{\left(\sqrt{E_1}+\sqrt{E_2}\right)^4}{M^4} - \frac{2\left(\sqrt{E_1}+\sqrt{E_2}\right)^4}{M^3} + \frac{\sqrt{E_1}\sqrt{E_2}\left(\sqrt{E_1}+\sqrt{E_2}\right)^2}{M^2} + \frac{\left(E_1+\sqrt{E_2}\sqrt{E_1}+E_2\right)\left(\sqrt{E_1}+\sqrt{E_2}\right)^2}{M} > 0\,.$$

For every $M > 4$ and $\sqrt{E_1 E_2} > \frac{3}{M}$,

$$p\left(-\frac{\sqrt{E_1}+\sqrt{E_2}}{2M}\right) = \frac{\left(\sqrt{E_1}+\sqrt{E_2}\right)^4}{16M^4} - \frac{\left(\sqrt{E_1}+\sqrt{E_2}\right)^4}{4M^3} + \frac{\left(E_1+4\sqrt{E_2}\sqrt{E_1}+E_2\right)\left(\sqrt{E_1}+\sqrt{E_2}\right)^2}{8M^2} + \frac{(E_1+E_2)\left(\sqrt{E_1}+\sqrt{E_2}\right)^2}{4M} - \frac{1}{4}\sqrt{E_1}\sqrt{E_2}\left(\sqrt{E_1}+\sqrt{E_2}\right)^2 < 0\,.$$

Hence, $p(\lambda)$ has a root between $-\frac{\sqrt{E_1}+\sqrt{E_2}}{2M}$ and $-\frac{\sqrt{E_1}+\sqrt{E_2}}{M}$.

It follows from the assumption $E_1 + E_2 = 1$ that $\sqrt{E_1}+\sqrt{E_2} \in [1, \sqrt{2}]$. Therefore, for sufficiently large M and every (E_1, E_2) such that $0.5 \geq \min\{\sqrt{E_1}, \sqrt{E_2}\} \geq \text{const} \cdot M^{-1}$, we have $-\rho_2 \sim r_1 M^{-1} \sim M^{-2}$. However, if $\min\{\sqrt{E_1}, \sqrt{E_2}\} \ll M^{-1}$, we have $-\rho_2 \leq M^{-1}\min\{\sqrt{E_1}, \sqrt{E_2}\} \ll M^{-2}$. In other words, $p_{1,1}$, the steady-state probability of (1, 1), does not differ from the rate of the first passage time to (1, 1) too much if and only if $\min\{\sqrt{E_1}, \sqrt{E_2}\}$ is at least $\sim M^{-1}$, as seen in Figure 12. Therefore, the prediction (6.1) is valid only if both $\sqrt{E_1}$ and $\sqrt{E_2}$ are above a certain threshold.

Remark 6.1. As a result, for the small particle system, the prediction made by Ref. 14 is only valid when the effect of low energy particles can be neglected. Let κ and t denote the size of the "bottleneck" and the time, respectively. We remark that one approach to neglect the effect of low energy particles is to rescale t by κ while letting $\kappa \to 0$, *before* letting $t \to \infty$. In this way, the stochastic energy exchange rate will approach to a strictly positive function almost everywhere as $\kappa \to 0$. Therefore, at the limit, the effect of low energy particles vanishes. Otherwise, if we study the asymptotic properties as $t \to \infty$ for any strictly positive κ, the effect of low energy particles cannot be ignored. In other words, the order of limits makes a significant difference here.

VII. NOTE ON NUMERICAL SIMULATIONS

Most numerical results in this paper are obtained from directed Monte Carlo simulations on parallel machines. The parallel random number generator used in our simulations

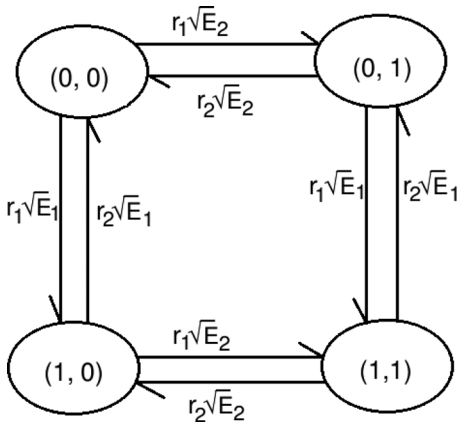

FIG. 13. Another CTMC model for a confined particle system.

comes from the library TRNG.[1] The main advantage of TRNG is that it guarantees the independence of random numbers generated by different threads. In addition, the nonlinear random generator used by TRNG has better performance than the standard Mersenne twister generator in many tests of randomness.[1] The period of the random number generator we choose is $\approx 4.61 \times 10^{18}$, which is at least $\sim 10^6$ times larger than the number of pseudorandom numbers used in our simulations.

The following Monte Carlo simulations are performed.

A. Simulation 1: Rate of mixing

The aim of this simulation is to compute the mixing rate of the big/small particle system. We are interested in the estimate of

$$C_{A,B}(t) := \left| \int_A P^t(x,B)\pi(\mathrm{d}x) - \pi(A)\pi(B) \right|$$

for some $A, B \subset \mathbf{\Omega}$.

As explained in Section IV, it is not practical to estimate $C_{A,B}$ directly for the small particle system. Instead, we compute the tail distribution of

$$\sigma_B := \inf_{t>0}\{\Phi_t \in B \,|\, \Phi_0 \text{ is uniformly distributed in } A\}\,.$$

We choose sets $A = \{x_1 \in [1, 1.5] \times [-0.25, 0.25];\ x_2 \in [-1.5, 1] \times [-0.25, 0.25]; |v_2|^2 < 0.01\}$ and $B = \{|v_2|^2 \geq 0.4\}$. 2×10^{10} initial values are uniformly chosen in A. The probability $\mathbb{P}[\sigma_B > t]$ is estimated at $t = \{0, 100, \ldots, 1 \times 10^7\}$. The total computation time is about 1.246×10^6 s on 32 CPUs. The same computation of σ_B is also carried out for the big particle system. The probability $\mathbb{P}[\sigma_B > t]$ is computed at $t = \{0, 1, \ldots, 200\}$. The total computation time is 12 420.9 s on 64 CPUs.

The rate of mixing is explicitly computed for the big particle system. We choose sets $A_0 = \{x_1 \in [1, 1.5] \times [-0.25, 0.25];\ x_2 \in [-1.5, 1] \times [-0.25, 0.25];\ |v_2|^2 < 0.1\}$ and $B_0 = \{0.4 \leq |v_2|^2 \leq 0.6\}$. The sample size is 1×10^{11}, of which Φ_0 is uniformly distributed in A_0. The mixing function $C_{A_0,B_0}(t)$ is calculated at $t = \{0, 1, \ldots, 50\}$. The total computation time is 554 298 s on 64 CPUs.

B. Simulation 2: Tail distribution of the conditional hitting time

The aim of this simulation is to estimate $R(E_1, E_2)$ with varying E_1 and E_2 in the big/small particle system from its conditional hitting time. The results obtained from this simulation are used in Figures 5, 12, and 11.

We first compute the tail distribution

$$p(t, E_2) := \mathbb{P}[\tau_B > t \,|\, \Phi_0 = \lambda_4|_\Gamma \times \delta(|v_1| - E_1) \times \delta(|v_2| - E_2)]$$

of the big/small particle system.

Twenty-eight different initial values of E_2 are chosen for the small particle system: $E_2 = \{0.5, 0.45, 0.4, 0.35, 0.3, 0.25, 0.2, 0.15, 0.1, 0.05, 0.02, 0.01, 0.005, 0.0025, 1 \times 10^{-3}, 5 \times 10^{-4}, 2.5 \times 10^{-4}, 1 \times 10^{-4}, 5 \times 10^{-5}, 2.5 \times 10^{-5}, 1 \times 10^{-5}, 5 \times 10^{-6}, 2.5 \times 10^{-6}, 1 \times 10^{-6}, 5 \times 10^{-7}, 2.5 \times 10^{-7}, 1 \times 10^{-7}, 2.5 \times 10^{-8}\}$. The sample size of each energy configuration is 5×10^8. The standard deviation of $p(t, E_2)$ can be estimated as

$$\mathrm{SD}(t, E_2) = \sqrt{\frac{1}{n}\hat{p}(t, E_2)(1 - \hat{p}(t, E_2))}\,,$$

where the estimator of $p(t, E_2)$, denoted by $\hat{p}(t, E_2)$, is the proportion of trajectories whose first energy exchange time is greater than t. $\hat{p}(t, E_2)$ is kept if and only if $\mathrm{SD}(t, E_2) \leq 0.01 \cdot \hat{p}(t, E_2)$. The total computation time is 361 630 s on 64 CPUs.

For the big particle system, twenty-nine different initial values of E_2 are chosen, which are the numbers listed above together with $E_2 = 0$. The sample size of each energy configuration is 2×10^9. $\hat{p}(t, E_2)$ is selected using the same criterion. The total computation time is 8820.27 s on 25 CPUs.

The rate $R(E_1, E_2)$, that is, the tail distribution of the conditional hitting time, is estimated as the negative slope of $\log(\hat{p}(t, E_2))$, as introduced above. Slopes are estimated from linear regressions. All 57 log-linear plots of $\hat{p}(t, E_2)$ form perfect straight lines. The relative errors of slopes are $<1\%$ for the big particle system and $<0.01\%$ for the small particle system at the 95% confidence level. See Figure 14 for examples of log-linear plots of $\hat{p}(t, E_2)$.

The waiting time for the first energy exchange from the uniform initial distribution can be estimated in the same way (i.e., $\Phi_0 = \pi$). Results obtained from this simulation are used in Figures 6 and 7. The sample size of the big particle system is 2×10^{10}; the total computation time is 2939.89 s on 25 CPUs. The sample size and total computation time of the small particle system are 8×10^{10} and 438 854 s (on 64 CPUs), respectively.

C. Simulation 3: Comparison of tails

The aim of this simulation is to verify that the conditional hitting time distribution and the conditional return time distribution have the same exponential tail, which justifies a well-defined stochastic energy exchange rate.

We start from a randomly chosen $\mathbf{x}_0$ and run the trajectory for a large number of steps to obtain the tail distribution of the return time. The simulation that produces Figure 8 compares the tails of $\Lambda(t)$ defined in Eq. (1) and e^{-t} for the big/small particle system. The stochastic energy exchange rate $R(E_1, E_2)$ is obtained from simulation 2 and a cubic spline interpolation. The number of particle-particle collisions in both trajectories is 1×10^8. The total computation time for the big particle system and the small particle system is 334.651 *s* and 43 225.3 *s* on a single CPU, respectively.

The simulation that produces Figure 9 compares tail distributions of conditional hitting time and that of conditional return time directly. We first collect samples $\{(E_1^{(i)}, E_2^{(i)}, t^i)\}_{i=1}^N$ from running a single trajectory. These samples are distributed into 1000 "bins" with size 5×10^{-4} based on the value of $\min\{E_1, E_2\}$. The corresponding exponential tails of conditional return time distributions for

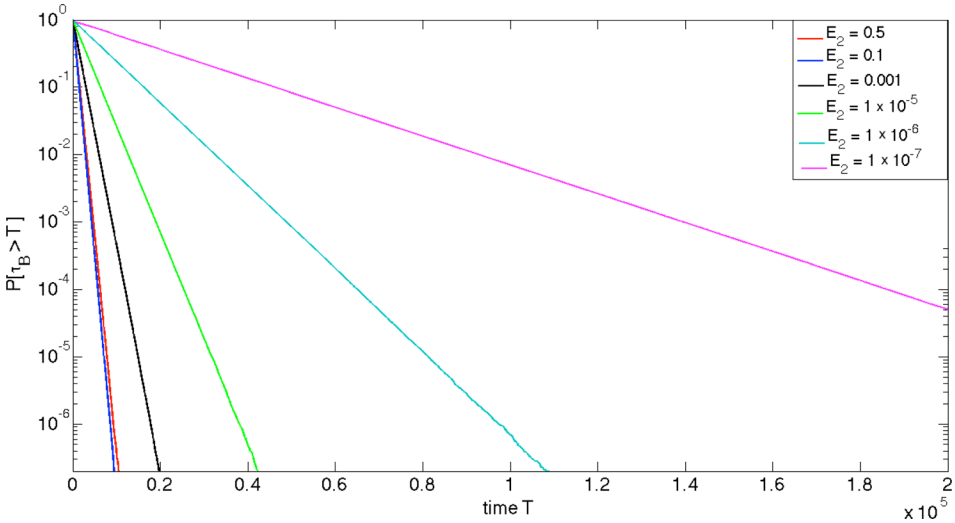

FIG. 14. $\hat{p}(t, E_2)$ in the log-linear plot. E_2 is taken to be 0.5, 0.1, 0.001, 1×10^{-5}, 1×10^{-6}, and 1×10^{-7}.

samples in each "bin" are computed in the same way as in simulation 2. Slopes of tails of conditional hitting time distributions, that is, $R(E_1, E_2)$, are also obtained from simulation 2. The number of particle-particle collisions in the trajectories of the big particle system and the small particle system is 1×10^9 and 5×10^8, respectively. The total computation time for those two cases is 5154.76 *s* and 209 824 *s* on a single CPU, respectively.

VIII. CONCLUSION

The geometric setting of a locally confined particle system can fundamentally change its statistical properties and the energy exchange regime at the cell-to-cell level. If a very slow particle in the system can hide from the others (small particle systems), the waiting time before its next energy exchange mainly depends on its own kinetic energy. As a result, starting from a class of initial distributions, the waiting time distribution to the next particle-particle collision, the convergence rate to equilibrium, and the mixing rate have only polynomial tails. In addition, our numerical evidence suggests that a well-defined stochastic energy exchange rate $R(E_1, E_2)$ exists and is $\sim\sqrt{\min\{E_1, E_2\}}$ as $\min\{E_1, E_2\} \to 0$. This scaling can be further qualitatively explained by a CTMC model.

In contrast, if the geometric configuration always allows fast particles to "activate" slow ones (big particle systems), the regime of energy exchange mainly depends on the total energy stored in adjacent cells. Exponential mixing rates and exponential convergence rates to the equilibrium are observed as expected. Our numerical simulations also confirm the existence of a stochastic energy exchange rate $R(E_1, E_2)$, which has the scaling $R(E_1, E_2) \sim \sqrt{E_1 + E_2}$.

In addition, we find that when particle-particle collisions are rare, that is, the "bottleneck" is narrow, the estimate $\hat{R}(E_1, E_2) \sim \sqrt{E_1 + E_2}$ in Ref. 14 is roughly reasonable unless $\min\{E_1, E_2\} \ll 1$. The gap at the low energy limit comes from a crucial hidden assumption in Ref. 14, which assumes a local thermal equilibrium of two adjacent cells is reached no later than the first particle-particle collision between them. According to the analysis of our CTMC approximation, this assumption is not valid if $\min\{E_1, E_2\}$ is smaller than a certain threshold. As explained in Section VI, one approach to close this gap is to change the order of limits.

In summary, whether or not stochastic modifications of locally confined particle systems preserve their main statistical features depends on many factors, geometry in particular. Stochastic modifications should be treated with care, especially when studying asymptotic statistical properties.

ACKNOWLEDGMENTS

The author thank Alexander Grigo, Kevin Lin, Peter Nandori, Herbert Spohn, and Lai-Sang Young for helpful discussions and valuable comments.

[1]H. Bauke, W. E. Brown, M. Fischler, J. Kowalkowski, M. Paterno, D. E. Knuth, W. H. Press, S. A. Teukolsky, W. T. Vetterling, B. P. Flannery *et al.*, *Tina's random number generator library*, 2011; available at http://numbercrunch.de.trng/.
[2]C. Bernardin and S. Olla, "Fourier's law for a microscopic model of heat conduction," J. Stat. Phys. **121**(3–4), 271–289 (2005).
[3]R. Bowen and J.-R. Chazottes, *Equilibrium States and the Ergodic Theory of Anosov Diffeomorphisms* (Springer, 1975), Vol. 470.
[4]L. Bunimovich, C. Liverani, A. Pellegrinotti, and Y. Suhov, "Ergodic systems of n balls in a billiard table," Commun. Math. Phys. **146**(2), 357–396 (1992).
[5]N. Chernov, "Limit theorems and Markov approximations for chaotic dynamical systems," Probab. Theory Related Fields **101**(3), 321–362 (1995).
[6]N. Chernov and R. Markarian, *Chaotic Billiards* (American Mathematical Society, 2006), Vol. 127.
[7]N. Chernov and L.-S. Young, in "Decay of correlations for Lorentz gases and hard balls," *Hard Ball Systems and the Lorentz Gas* (Springer, 2000), pp. 89–120.
[8]J. R. Dorfman, *An Introduction to Chaos in Nonequilibrium Statistical Mechanics* (Cambridge University Press, 1999), Vol. 14.
[9]J.-P. Eckmann and L.-S. Young, "Nonequilibrium energy profiles for a class of 1-d models," Commun. Math. Phys. **262**(1), 237–267 (2006).
[10]A. C. M. Freitas, J. M. Freitas, and M. Todd, "The extremal index, hitting time statistics and periodicity," Adv. Math. **231**(5), 2626–2665 (2012).
[11]A. C. M. Freitas, J. M. Freitas, M. Todd, and S. Vaienti, "Rare events for the manneville-pomeau map," Ann. Probab **43**(4), 1663–1711 (2015).
[12]P. Gaspard, *Chaos, Scattering and Statistical Mechanics* (Cambridge University Press, 2005), Vol. 9.
[13]P. Gaspard and T. Gilbert, "Heat conduction and Fourier's law by consecutive local mixing and thermalization," Phys. Rev. Lett. **101**(2), 020601 (2008).

[14]P. Gaspard and T. Gilbert, "Heat conduction and Fourier's law in a class of many particle dispersing billiards," New J. Phys. **10**(10), 103004 (2008).
[15]P. Gaspard and T. Gilbert, "On the derivation of Fourier's law in stochastic energy exchange systems," J. Stat. Mech.: Theory Exp. **2008**(11), P11021.
[16]P. Gaspard and T. Gilbert, "Heat transport in stochastic energy exchange models of locally confined hard spheres," J. Stat. Mech.: Theory Exp. **2009**(08), P08020.
[17]P. Gaspard and T. Gilbert, "A two-stage approach to relaxation in billiard systems of locally confined hard spheres," Chaos **22**(2), 026117 (2012).
[18]T. Gilbert, "On the waiting time distributions of systems of locally confined particles with rare interactions," J. Stat. Mech.: Theory Exp. **2011**(06), P06015.
[19]A. Grigo, K. Khanin, and D. Szasz, "Mixing rates of particle systems with energy exchange," Nonlinearity **25**(8), 2349 (2012).
[20]N. Haydn, Y. Lacroix, and S. Vaienti, "Hitting and return times in ergodic dynamical systems," Ann. Probab. **2005**, 2043–2050.
[21]N. T. A. Haydn, "Entry and return times distribution," Dyn. Syst. **28**(3), 333–353 (2013).
[22]M. Hirata, "Poisson law for axiom a diffeomorphisms," Ergodic Theory Dyn. Syst. **13**(03), 533–556 (1993).
[23]M. Hirata, B. Saussol, and S. Vaienti, "Statistics of return times: A general framework and new applications," Commun. Math. Phys. **206**(1), 33–55 (1999).
[24]C. Kipnis, C. Marchioro, and E. Presutti, "Heat flow in an exactly solvable model," J. Stat. Phys. **27**(1), 65–74 (1982).
[25]R. Klages and C. Dellago, "Density-dependent diffusion in the periodic Lorentz gas," J. Stat. Phys. **101**(1–2), 145–159 (2000).
[26]R. Klages, *Microscopic Chaos, Fractals and Transport in Nonequilibrium Statistical Mechanics* (World Scientific Singapore, 2007), Vol. 40.
[27]G. Knight and R. Klages, "Capturing correlations in chaotic diffusion by approximation methods," Phys. Rev. E **84**(4), 041135 (2011).
[28]R. Lefevere, M. Mariani, and L. Zambotti, "Macroscopic fluctuation theory of aerogel dynamics," J. Stat. Mech.: Theory Exp. **2010**(12), L12004.
[29]Y. Li and L.-S. Young, "Existence of nonequilibrium steady state for a simple model of heat conduction," J. Stat. Phys. **152**(6), 1170–1193 (2013).
[30]Y. Li and L.-S. Young, "Nonequilibrium steady states for a class of particle systems," Nonlinearity **27**(3), 607 (2014).
[31]B. Pitskel, "Poisson limit law for Markov chains," Ergodic Theory Dyn. Syst. **11**(03), 501–513 (1991).
[32]L. Rey-Bellet and L.-S. Young, "Large deviations in non-uniformly hyperbolic dynamical systems," Ergodic Theory Dyn. Syst. **28**(02), 587–612 (2008).
[33]Z. Rieder, J. L. Lebowitz, and E. Lieb, "Properties of a harmonic crystal in a stationary nonequilibrium state," J. Math. Phys. **8**(5), 1073–1078 (1967).
[34]M. Sasada, in "On the spectral gap of the Kac walk and other binary collision processes on d-dimensional lattice," *Symmetries, Integrable Systems and Representations* (Springer, 2013), pp. 543–560.
[35]M. Sasada, "Spectral gap for stochastic energy exchange model with non-uniformly positive rate function," preprint arXiv:1305.4066 (2013).
[36]Y. Grigor'evich Sinai, "Dynamical systems with elastic reflections. ergodic properties of dispersing billiards," Usp. Mat. Nauk. **25**(2), 141–192 (1970).
[37]T. Yarmola, "Sub-exponential mixing of random billiards driven by thermostats," Nonlinearity **26**(7), 1825 (2013).
[38]L.-S. Young, "Statistical properties of dynamical systems with some hyperbolicity," Ann. Math. **147**, 585–650 (1998).
[39]L.-S. Young, "Recurrence times and rates of mixing," Israel J. Math. **110**(1), 153–188 (1999).